Path Following with Reduced Off-Tracking for Multibody Wheeled Vehicles

Claudio Altafini

Abstract— **Our purpose is to provide a formulation of the path following problem for multibody kinematic wheeled vehicles aiming to keep the whole vehicle at a reduced distance from a given path, i.e. to reduce the off-tracking distance of the vehicle from the path. In the proposed setting, the stabilization problem for paths of constant curvature is locally solvable by a simple linear feedback law. In order to quantify how much cumbersome a vehicle is along a given path, we provide two different estimates of the off-tracking bound, i.e. of the minimal clearance that has to be left around the path in order for the vehicle to pass through in case of perfect tracking. Experimental results on a miniature multibody vehicle are reported.**

Keywords— **Multibody wheeled vehicle, Path following, Off-tracking distance, Feedback linearization.**

I. Introduction

The main difference between the trajectory tracking and path following problems for wheeled vehicles is in the idea of tracking error that they induce, see Chapter 8 of [9] or [8] for a survey. In the trajectory tracking, a reference value of the entire state of the system is given [16], [22], while in the path following problem only a curve in the plane is provided as reference but not a function of time. This implies that there is no concern on the longitudinal dynamics, i.e. on how fast the path is covered, but only on the lateral dynamics specified by an appropriate notion of *error distance*. For kinematic wheeled vehicles, several different path tracking criteria have been proposed. A possible approach is, for example, to study the problem as a variant of the trajectory tracking problem, where a virtual vehicle is placed on the path to follow. This leads to define the tracking error as the distance between a point on the real vehicle and the corresponding point on the virtual vehicle and to prove convergence of the real robot to the virtual one. In [13] for example, this distance is a look-ahead distance, obtained by means of an appropriate sensor like a camera; alternatively, in [11] a special parameterization based on velocity scaling is used.

However, all the research that we are aware of, deal with the problem of path following for one single given point of the vehicle: either the middle point of the front wheels or the middle point of the last axle (like in the flatness or chained form based methods) or some intermediate point, like the center of gravity of the vehicle (see e.g. the work [14]). For multiaxis vehicles, a number of situations in which one single guidepoint is not enough were presented in [1], [4]. They all have in common the need of maintaining the *whole* vehicle at a reduced distance from the path and they can be represented by a different tracking error condition, based not on the error distance of one single point but on the sum of the error distances of the middle points of all the axles of the vehicle. We call this the *off-tracking distance*. For the so-called *general n-trailer*, in order to keep track of $n+1$ distances, we use $n+1$ moving frames, also called Frenet frames [18]. Such lateral distances are meant to be measurable quantities, see for example the case of the underground mining truck [10] where wall detecting sensors are available. In other applications, multiple edge-detection sensors, like cameras, can be available. The use of multiple sensors for the lateral distance is documented for example in [15] for different purposes.

The off-axle hooking of a general n-trailer seems to spoil the nice properties of the standard n-trailer like flatness [12] and chained form [21], making also the problem of stabilizing to a path more complex, as full state feedback linearization cannot be achieved. Stabilization problems for general n-trailers are studied for example in [6], [17]. In particular, in [6] a virtual reference vehicle is used in which the "ghost" vehicle is the corresponding n-trailer without kingpin hitching, for which exact feedback linearization holds.

In our case, for paths of constant curvature, local asymptotic stability can be achieved by means of linear controllers based on Jacobian linearization. In particular, for forward motion the simplest control law is a first order high gain output feedback. Only the proof of stability is hard because the simultaneous use of many reference frames implies that there is no explicit expression for the linearization. In fact we need to resort to the input-optput feedback linearization techniques used in [3]. It is important to emphasize that, unlike for example in [20], the complexity of the controller remains the same regardless of the number of trailers.

We show that for the case of perfect tracking the distances that we obtain for the midpoints of the axles, corresponding to the notion of the system on the output zeroing manifold, provide an *off-tracking bound*, i.e. an estimate of what is the *minimal width of the road* that has to be left on both sides of the planned path in order to have the vehicle passing through the obstacles (see [7] for a similar problem formulation). This off-tracking bound based on the zero dynamics is compared with a simpler one corresponding to the steady state off-tracking of the maximum of curvature encountered along the path.

The simple high gain output feedback controller proposed in the paper is tested in a practical experiment on a miniaturized (1:16 scale) general 3-trailer. Even in presence of realistic problems like saturation and of limited measurement information, it is shown how the "reduced off-tracking" notion is implementable in practice.

We would like to stress the fact that the whole analysis is *local* and to point out that, due to the singularities of the Frenet frame representation, there is no way to formally prove a well-behaved transient even for admissible (wrong) initial conditions that are too close to the limits of the region of attraction.

C. Altafini was with the Division of Optimization and Systems Theory, Royal Institute of Technology SE-10044, Stockholm, Sweden; he is now with SISSA-ISAS International School for Advanced Studies, via Beirut 4, 34014 Trieste, Italy; e-mail: `altafini@sissa.it`

II. Kinematic model for the general n-trailer and Frenet frames

Notation, modeling assumptions and equations are the same as [3] and are briefly recapitulated here. The legenda for the symbols used below is (see also Fig. 1):
n = number of trailers
m = number of off-hitching ($m < n$)
$n_1, \ldots, n_m$ = indexes of the axles having off-hitching ($n_j < n_{j+1}$, $n_m < n$, $M_{n_j} \neq 0$)
P_i = midpoint of the i-th axis
L_i = distance between P_i and the hitching point in front of it ($L_i \geq 0$)
M_i = distance between P_i and the hitching point behind it ($M_i \geq 0$)
v_i = longitudinal velocity of P_i
θ_i = absolute orientation angle
$\beta_i = \theta_{i-1} - \theta_i$
γ = reference path
κ_γ = curvature of the path
Γ_i = orthogonal projection of P_i on γ
s_{γ_i} = arclenght coordinate of the i-th curvilinear frame
θ_{γ_i} = orientation angle of the i-th frame with respect to the cartesian axes
z_i = distance between P_i and Γ_i
$\tilde{\theta}_i = \theta_i - \theta_{\gamma_i}$

It was shown in [18], [19] that a frame moving on the path can be useful to locally describe a point moving on the plane, instead of a fixed frame. This moving frame, called the Frenet frame, only requires to describe the distance between the path and the vehicle, whereas the length covered along the path can be neglected. An advantage of the Frenet frame is that it naturally decouples the lateral dynamics from the longitudinal one, providing a measure of the error from the path in terms of the (signed) distance z_i; a disadvantage is that the parameterization used is intrinsically not global for paths of nonnull curvature. In the Frenet frame, the point P_i is represented by z_i and by the relative orientation angle $\tilde{\theta}_i$. In our case, we consider $n+1$ Frenet frames moving on γ and anchored at Γ_i. The tracking criterion proposed consists in taking the *sum* of the signed distances:

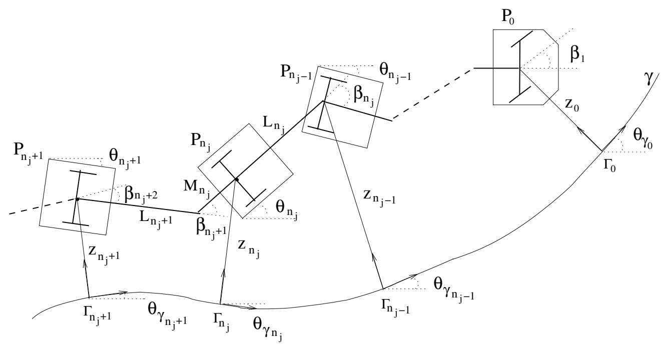

Fig. 1. The general n-trailer and the Frenet frames.

$$y = \sum_{i=0}^{n} z_i \to 0 \tag{1}$$

Of the two inputs of the kinematic n-trailer, the steering speed $\omega = \dot{\beta}_1$ and the translational speed of one of the P_i, for example v_n, only ω is considered for the path following problem, thus obtaining a system with drift. Calling $\boldsymbol{p}_i = \left[s_{\gamma_i}\ z_i\ \tilde{\theta}_i,\ \beta_i\right]^T$, the whole configuration state is represented by $\boldsymbol{p} = \left[\boldsymbol{p}_n,\ \boldsymbol{p}_{n-1},\ \ldots, \boldsymbol{p}_0\right]^T$, $\boldsymbol{p} \in \mathcal{D}$, and the dynamic equations of the system are:

$$\dot{\boldsymbol{p}} = \begin{bmatrix} \mathcal{F}_n \\ \vdots \\ \mathcal{F}_2 \\ \mathcal{F}_1 \\ \mathcal{F}_0 \end{bmatrix} + \begin{bmatrix} 0 \\ \vdots \\ 0 \\ \mathcal{G}_1 \\ \mathcal{G}_0 \end{bmatrix} \omega = \mathcal{F}(\boldsymbol{p}) + \mathcal{G}\omega \tag{2}$$

together with the output equation:

$$y = [0100\ 0100 \ldots 0100\ 010]\boldsymbol{p} \triangleq \mathcal{H}\boldsymbol{p} \tag{3}$$

The domain of definition $\mathcal{D}$ and the singular locus are discussed in [2]. The drift terms $\mathcal{F}_k = \mathcal{F}_k\left(\boldsymbol{p}_k,\ \underline{\beta}_{k+1},\ \kappa_\gamma(s_{\gamma_k}),\ v_n\right)$ (where $\underline{\beta}_k = [\beta_k \ldots \beta_n]$) have different expressions depending on whether the axle has off-hitching or not. Calling $c_k \triangleq \left(1 + \frac{M_k}{L_k}\tan\beta_k \tan\beta_{k+1}\right)$, they can be summarized as:

$$\mathcal{F}_{n_j+i} = v_{n_j+i}\begin{bmatrix} \frac{\cos\tilde{\theta}_{n_j+i}}{1-\kappa_\gamma(s_{\gamma_{n_j+i}})z_{n_j+i}} \\ \sin\tilde{\theta}_{n_j+i} \\ \frac{\tan\beta_{n_j+i} - \frac{M_{n_j+i-1}}{L_{n_j+i-1}}\tan\beta_{n_j+i-1}}{L_{n_j+i}c_{n_j+i-1}} - \frac{\cos\tilde{\theta}_{n_j+i}\,\kappa_\gamma(s_{\gamma_{n_j+i}})}{1-\kappa_\gamma(s_{\gamma_{n_j+i}})z_{n_j+i}} \\ \frac{\tan\beta_{n_j+i-1}}{L_{n_j+i-1}\cos\beta_{n_j+i}} - \frac{\tan\beta_{n_j+i}}{L_{n_j+i}} + \frac{M_{n_j+i-1}\tan\beta_{n_j+i-1}}{L_{n_j+i}L_{n_j+i-1}} \end{bmatrix} \tag{4}$$

$j \in \{0, 1, \ldots, m\}$, $i \in \{1, \ldots, n_{j+1} - n_j\}$, $n_0 = 0$, $n_{m+1} = n$, where

$$v_{n_j+i} = \frac{v_n}{\prod_{k=j+1}^{m} c_{n_k} \prod_{k=n_j+i+1}^{n} (\cos\beta_k)} \tag{5}$$

$j \in \{0, 1, \ldots, m\}$, $i \in \{1, 2 \ldots, n_{j+1} - n_j\}$. For the points P_1 and P_0, the equations are function also of the steering input ω. Assuming $n_1 > 1$, we get

$$\mathcal{F}_1 = v_1 \begin{bmatrix} \frac{\cos\tilde{\theta}_1}{1-\kappa_\gamma(s_{\gamma_1})z_1} \\ \sin\tilde{\theta}_1 \\ \frac{\tan\beta_1}{L_1} - \frac{\cos\tilde{\theta}_1\,\kappa_\gamma(s_{\gamma_1})}{1-\kappa_\gamma(s_{\gamma_1})z_1} \\ 0 \end{bmatrix}, \quad \mathcal{G}_1 = \begin{bmatrix} 0 \\ 0 \\ 0 \\ 1 \end{bmatrix} \tag{6}$$

In P_0 there is no equation for β (i.e. $\boldsymbol{p} = \left[s_{\gamma_0}\ z_0\ \tilde{\theta}_0\right]^T$):

$$\mathcal{F}_0 = v_0 \begin{bmatrix} \frac{\cos\tilde{\theta}_0}{1-\kappa_\gamma(s_{\gamma_0})z_0} \\ \sin\tilde{\theta}_0 \\ \frac{\sin\beta_1}{L_1} - \frac{\cos\tilde{\theta}_0\,\kappa_\gamma(s_{\gamma_0})}{1-\kappa_\gamma(s_{\gamma_0})z_0} \end{bmatrix}, \quad \mathcal{G}_0 = \begin{bmatrix} 0 \\ 0 \\ 1 \end{bmatrix} \tag{7}$$

Again, v_1 and v_0 are calculated using (5).

The number of states is then $4(n+1)-1$ while the number of independent variables in the n-trailer problem is $n+3$. Therefore we must impose constraints on the state space expressing the redundancy introduced by the use of $n+1$ frames. Except for the trivial cases, these constraints cannot be written in a purely algebraic form, since they depend on line integrals. If E is a generic point of the body segment $[P_i,\ P_{i-1}]$ and dl is the increment along the body, they can be written as:

$$s_{\gamma_{i-1}} = s_{\gamma_i} + \int_0^{L_i+M_i} \frac{\cos\tilde{\theta}_E(l)dl}{1-\kappa_\gamma(s_{\gamma_E}(l))z_E(l)} \tag{8}$$

$$\tilde{\theta}_{i-1} = \tilde{\theta}_i + \beta - \int_0^{L_i+M_i} \kappa_\gamma(s_{\gamma_E}(l))\dot{s}_{\gamma_E}(l)dl \tag{9}$$

$$z_{i-1} = z_i + \int_0^{L_i+M_i} \sin\tilde{\theta}_E(l)dl \tag{10}$$

where $dl = v_l\, dt$ with v_l acquiring the meaning of the "velocity" with which the point E moves along the body of the vehicle. If the path to follow is a straight line, for example the x axis on the cartesian coordinates ($s_\gamma = x$), then the Frenet frames reduces to cartesian frames. Equations (8)-(10) then trivialize to:

$$s_{\gamma_{i-1}} = s_{\gamma_i} + L_i\cos\theta_i$$
$$\theta_{\gamma_i} = 0$$
$$z_{i-1} = z_i + L_i\sin\theta_i$$

and the extra variables can be eliminated in a straightforward manner. In general, when κ_γ varies, the constraints are not anymore integrable, but also with $\kappa_\gamma = \text{const} \neq 0$ their explicit expression is very difficult to calculate.

III. Following a path of constant curvature

In this Section, we will focus on paths of constant curvature $\kappa_\gamma = const \neq 0$. In this case, from (4), the variables s_{γ_i} can be dropped from the model and the steady state corresponds to have the angles $\beta_i = const$ $\forall\, i \in \{1, 2, \ldots, n\}$ and such that $y = 0$. Also the $\tilde{\theta}_i$ tend to a constant value (the origin): in fact, at steady state, the points P_i rotate around circles concentric with the path γ. Linearizing (2), in a neighborhood of the origin the derivative of the distance z_i can be thought of as:

$$\dot{z}_i = v_i\sin\tilde{\theta}_i \simeq v_i\tilde{\theta}_i \tag{11}$$

This fact allows us to locally identify a partial state feedback based on both z_i and $\tilde{\theta}_i$ with a dynamic controller based only on the distances z_i.

Since the constraints (8)-(10) cannot be easily handled, not even with $\kappa_\gamma = const$, we will simply drop them and study stability on the augmented configuration space. If stability is found on this bigger manifold, then stability will also hold in the original submanifold satisfying the constraints.

We need to distinguish between forward and backward motion. Notoriously, the path following problem is much easier in the forward direction than in the other one. Here only the first is analyzed; for the second case we refer to [5]. Locally, the sign of v_n univocally identifies the direction of motion.

A. Forward motion

If we exclude the subsystem $\dot{\beta} = \omega$ which is only critically stable, for the forward motions the rest of the system is open-loop asymptotically stable. In this case, a dynamic output feedback is enough to achieve local asymptotic stability. Since the system has relative degree equal to 2 (see Section IV), the feedback has to include a derivative term of the output.

Calling $\boldsymbol{q}$ the $3(n+1)-1$ state vector obtained from $\boldsymbol{p}$ neglecting s_{γ_i}, we can rewrite the system (2)-(3) as:

$$\dot{\boldsymbol{q}} = \overline{\mathcal{F}}(\boldsymbol{q}) + \overline{\mathcal{G}}\,\omega \tag{12}$$

$$y = \overline{\mathcal{H}}\boldsymbol{q} \tag{13}$$

Proposition 1: When $v_n > 0$, there exist constant gains $k_1 < 0$ and $k_2 < 0$ such that the dynamic output feedback

$$\omega = k_1 y + k_2\dot{y} \tag{14}$$

locally asymptotically stabilizes the system (12)-(13) to a path of constant curvature $\kappa_\gamma \neq 0$, with κ_γ such that the algebraic equation

$$r_n + \sum_{i=0}^{n}\sqrt{r_n^2 + \sum_{j=1}^{n-1}\left(L_{j+1}^2 - M_j^2\right)} = \frac{n+1}{|\kappa_\gamma|} \tag{15}$$

admits a solution for some $r_n \geq 0$.

The most straightforward way to prove local stability is normally through the Lyapunov indirect method. At the equilibrium, each of the points P_i follows a circle concentric with the circular path γ. The radius r_i of the corresponding circle depends on κ_γ and on the configuration of the vehicle. We have the following recursive relation between the radii r_i and r_{i+1}: $r_i = \sqrt{r_{i+1}^2 + L_{i+1}^2 - M_i^2}$ or, in terms of the radius of the last trailer:

$$r_i = \sqrt{r_n^2 + \sum_{j=1}^{n-1}\left(L_{j+1}^2 - M_j^2\right)} \tag{16}$$

If $r_\gamma = 1/|\kappa_\gamma|$ is the radius of the path, the steady state condition

$$y_e = \sum_{i=0}^{n} z_{i_e} = \sum_{i=0}^{n}(r_\gamma - r_i) = 0 \tag{17}$$

implies that r_n can be found by solving the algebraic relation (15). For the common case $L_i \geq M_i$, the midpoint of the last trailer P_n is the one that "cuts" the curve the most. Therefore, a well-defined equilibrium for $\boldsymbol{q}$ exists only if $r_n \geq 0$. $r_n = 0$ is the extreme situation of the n-trailer rotating in circles with P_n standing still. Although the existence and uniqueness of the equilibrium point is guaranteed under the above conditions, it is an elementary algebraic fact that in an equation like (15) the square roots cannot be eliminated if $n \geq 3$. The consequence is that one has to resort to a numerical solution in order to find the value of r_n. From eq. (16), the same type of compatibility reasoning as $r_n \geq 0$ implies that the arguments of all the n square roots have to be positive. Due to the lack of analytic solution for (15), it is not possible to obtain a formal proof of the claim made in the proposition at this stage by using the Jacobian linearization, as an explicit expression of the state matrix (and therefore of its determinant) is lacking. A formal proof of Proposition 1 will be obtained in Section IV after analyzing the zero dynamics associated with the tracking error (1). The Jacobian linearization $\overline{\mathcal{F}}_e = \left.\frac{\partial \mathcal{F}}{\partial \boldsymbol{q}}\right|_{\boldsymbol{q}=\boldsymbol{q}_e}$ allows only to *numerically verify* that the reduced system (12)-(13) is Hurwitz stabilizable around the following equilibrium point:

$$\boldsymbol{q}_e = \left[z_{n_e}\ \tilde{\theta}_{n_e}\ \beta_{n_e} \dots z_{1_e}\ \tilde{\theta}_{1_e}\ \beta_{1_e}\ z_{0_e}\tilde{\theta}_{0_e}\right]^T \tag{18}$$

where

$$\begin{aligned} \beta_{i_e} &= \arctan\left(\frac{L_i\kappa_\gamma}{1-\kappa_\gamma z_{i_e}}\right) + \arctan\left(\frac{M_{i-1}\kappa_\gamma}{1-\kappa_\gamma z_{i-1_e}}\right) \quad (19)\\ z_{i_e} &= r_\gamma - r_i \\ \tilde{\theta}_{i_e} &= 0 \end{aligned}$$

If v_{i_e} are the velocities of the points P_i at $\boldsymbol{q}_e$ the matrix

$$\overline{\mathcal{H}}_2 = \begin{bmatrix} 1 & 0 & 0 & 1 & 0 & 0 & \dots & 1 & 0 & 0 \\ 0 & v_{n_e} & 0 & 0 & v_{n-1_e} & 0 & \dots & 0 & v_{0_e} & 0 \end{bmatrix}$$

can be used to transform the control law (14) into the (locally equivalent) partial state feedback $\omega = [k_1\ k_2]\overline{\mathcal{H}}_2\boldsymbol{q}$ by using eq. (11) and to numerically compute the values of k_1^* and k_2^* such that for $k_1 < k_1^* < 0$ and $k_2 < k_2^* < 0$ the matrix $\overline{\mathcal{F}}_e + \overline{\mathcal{G}}[k_1\ k_2]\overline{\mathcal{H}}_2$ is Hurwitz. In Section IV it will be shown that such an output feedback law admits the interpretation of high gain output feedback.

B. Comparison with the standard path following technique

The system (2)-(3) is a SISO system from steering input to tracking error. If $M_0 = 0$, its relative degree is well-defined and equal to 2 for any number of off-axle connections. If instead we take as guidepoint the midpoint of the rear axle of the vehicle and as corresponding tracking error

$$y = z_n \to 0 \tag{20}$$

like in [20], the relative degree of the system is $n - m + 1$, which says that the input-state feedback linearizability is lost, due to the kingpin hitching. This implies that the nice properties of flatness and chained form are also lost for the system. The different relative degree reflects a difference in the structure of the simplest possible controller needed to stabilize the system. In fact, for (20) a dynamic output feedback of order $n - m + 1$ is required:

$$\omega = \sum_{i=0}^{n-m+1} k_i y^{(i)} \tag{21}$$

IV. Input-output feedback linearization

The material of this Section overlaps with [3], Section III. To input-output feedback linearize the system it is enough to derive the output (3) twice and cancel the corresponding dynamics by means of a change of input. Assume $M_0 = M_1 = 0$ and call $\mathfrak{p}$ the state obtained from $\boldsymbol{p}$ excluding β_1 and $\tilde{\theta}_0$.

The zero dynamics is obtained confining the dynamics of the system to the Output-Zeroing Manifold $Z^* = \{\boldsymbol{p} \in \mathcal{D}\ s.t.\ y = \dot{y} = \ddot{y} = 0\}$ and it is obtained, for example, eliminating the variables z_0 and $\tilde{\theta}_0$ by means of

$$z_0 = -\sum_1^n z_i \tag{22}$$

$$\tilde{\theta}_0 = \arcsin\left(-\sum_{j=0}^{m}\sum_{i=1}^{n_{j+1}-n_j}\frac{v_n \sin\tilde{\theta}_{n_j+i}}{v_0\prod_{k=j+1}^{m} c_{n_k}\prod_{k=n_j+i+1}^{n}\cos\beta_k}\right) \tag{23}$$

Any output feedback of the form

$$u = k_1 y + k_2 \dot{y} \tag{24}$$

with $k_1 < 0$, $k_2 < 0$ is a locally asymptotically stabilizer for the resulting chain of integrators obtained applying the prefeedback of eq. (8) of [3].

Now the local asymptotic stability of the zero dynamics can be proven for a path of constant curvature.

Proposition 2: For forward motion, the zero dynamics of the n-trailer system (2)-(3) is locally exponentially stable along paths of constant curvature.
See Appendix A for a proof alternative to that appearing in [3].

With the result of Proposition 2, we can now straightforwardly obtain the proof of Proposition 1.

Proof of Proposition 1. The zero dynamics of the original nonlinear system being locally exponentially minimum phase together with the well-defined relative degree $r = 2$ is a sufficient condition for the existence of a high gain dynamic output feedback that locally asymptotically stabilizes the system. Hence also for the linearized system there exists $k_1^* < 0$ and $k_2^* < 0$ such that for $k_1 < k_1^*$ and $k_2 < k_2^*$ the matrix $\overline{\mathcal{F}}_e + \overline{\mathcal{G}}[k_1\ k_2]\overline{\mathcal{H}}_2$ is Hurwitz. ■

The property vanishes for backward motion, because the zero dynamics is not anymore locally minimum phase.

V. Zero dynamics and off-tracking bounds

We would like to have a way to calculate the minimal width of a road, i.e. how much clearance has to be left around a given path in order to make sure that the robot can pass through the obstacles, at least in the very simplificative case of perfect output tracking and of no error for the initial conditions on Z^*. On Z^*, n of the dynamic equations of the zero dynamics are described by the evolution of the orthogonal distances z_i, $i = 1, \dots, n$. The missing distance z_0 can be recovered from eq. (22). We take the maximum of z_i as measure of off-tracking.

The integral curves on Z^* that we obtain are only function of the curvature κ_γ and of the geometry of the vehicle. The value of the z_i at s_γ is then only function of the curvature κ_γ between the curvilinear abscissæ s_{γ_0} and s_{γ_n}:

$$z_i(s_\gamma) = z_i\left[\kappa_{\gamma_0}(s_\gamma),\, \kappa_{\gamma_n}(s_\gamma)\right] = z_i\left(\kappa_\gamma[s_{\gamma_0},\, s_{\gamma_n}]\right) \qquad (25)$$

Therefore we can build an "envelope" around the path by taking the maximum and minimum of the z_i for each s_γ. The explicit analytic expression of the dynamics of the z_i on Z^* is quite involved also for the low dimensional cases. However a numerical simulation showing the off-tracking envelopes is quite easy to produce. Assume we can model $\kappa_\gamma = \kappa_\gamma(s_{\gamma_i})$ as the output of an exogenous dynamical system by taking s_{γ_i} as independent variable:

$$\kappa'_{\gamma_i} = \frac{d\kappa_{\gamma_i}}{ds_{\gamma_i}} = \gamma\left(\kappa_{\gamma_i}\right) \qquad i = 0, 1, \dots n \qquad (26)$$

The curvature has $n + 1$ entries in the system equations, all described by the same differential equation (26) but with different initial conditions. The complete exogenous system in the time independent scale is $\kappa'_\gamma = \Gamma(\kappa_\gamma)$ where $k_\gamma = \left[k_{\gamma_n} \dots k_{\gamma_1}\, k_{\gamma_0}\right]^T$. The matrix $\Gamma(\cdot)$ is $\Gamma\left(\kappa_\gamma\right) = \mathrm{diag}\left[\gamma\left(\kappa_{\gamma_n}\right) \;\; \dots \;\; \gamma\left(\kappa_{\gamma_0}\right)\right]$ and the independent variable is s_γ. The entire system (2)-(3) can be transformed into the time-independent scale by taking the projection of the (known) velocity v_n on the path: $v_\gamma = \dot{s}_\gamma = v_n \cos\tilde{\theta}_n / \left(1 - \kappa_\gamma(s_\gamma) z_n\right)$. The system can be rescaled accordingly in terms of the increment in the new independent variable $ds_\gamma = v_\gamma dt$. The maximum of the off-tracking envelope is calculated by the following problem:

$$\begin{aligned} z_{max_1} = \quad & \max_{s_\gamma \in [0,\, S_\gamma]} \{ |\, z_i \,| \quad i = 0, 1, \dots, n\} \qquad (27) \\ s.t. \qquad & \underline{p}' = \underline{\mathcal{F}}\left(\underline{p},\, \kappa_\gamma\right) - \frac{\underline{\mathcal{G}}(\underline{p}) L^2_{\underline{\mathcal{F}}} \underline{\mathcal{H}} \underline{p}}{L_{\underline{\mathcal{G}}} L_{\underline{\mathcal{F}}} \underline{\mathcal{H}} \underline{p}} \\ & \kappa'_\gamma = \Gamma(\kappa_\gamma) \end{aligned}$$

where the underlined symbols replace the corresponding symbols of the system (2)-(3) in the time-independent scale. Solving this optimization problem can be computationally expensive. We suggest here a numerically simpler procedure, based on seeking the maximum of curvature $\kappa_{\gamma_{max}}$, computing the corresponding equilibrium point as in (17) and taking the maximum (in absolute value) of the corresponding lateral distance $|z_i|$. It is assumed that among the z_i, such maximum is achieved in one of the two extremities of the n-trailer: $\max\{|z_n|, |z_0|\}$. Consider, for example, $|z_n| > |z_0|$. The constant value that gives an upper bound to the off-tracking envelopes is

$$z_{max_2} = \frac{1 - r_{n_{max}} \kappa_{\gamma_{max}}}{\kappa_{\gamma_{max}}} \qquad (28)$$

where $\kappa_{\gamma_{max}} = \max_{s_\gamma \in [0,\, S_\gamma]} \kappa_\gamma(s_\gamma)$ and $r_{n_{max}}$ is obtained solving the algebraic equation (15). From above, the bound z_{max_2} is reached if κ_γ stays at $\kappa_{\gamma_{max}}$ for at least an interval of length $\left[s_{\gamma_{0_e}},\, s_{\gamma_{n_e}}\right]$ where $s_{\gamma_{0_e}}$ and $s_{\gamma_{n_e}}$ are the curvilinear abscissae at the equilibrium corresponding to some $s_\gamma \in [0,\, S_\gamma]$, otherwise the bound becomes conservative. For a path of constant curvature, the two off-tracking bounds z_{max_1} and z_{max_2} coincide.

VI. Experimental set-up

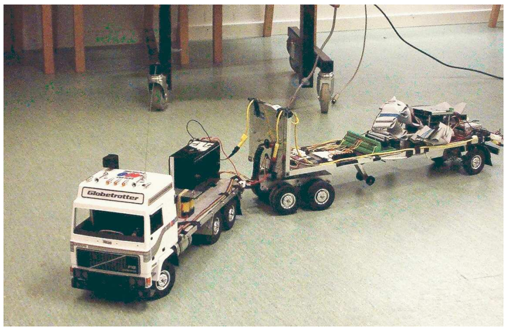

Fig. 2. The multibody vehicle used in the experiments.

The experimental platform shown in Fig. 2 is equipped with optical encoders on both wheels of the second and fourth axle (i.e. on P_1 and P_3), which allow for an incremental measurements of the distances z_1 and z_3, and potentiometers to measure the relative orientation angles β_1, β_2 and β_3. The signals were read at a frequency of 2kHz. This frequency and the 500 pulse shaft ensured a maximum speed of about 0.2 m/s which was sufficient for our application. Due to the lack of odometry information on P_0 and P_2, we replace the tracking criterion (1) with the simpler one $y = z_1 + z_3$. None of the consideration concerning the off-tracking is essentially modified by such change.

The vehicle of Fig. 2 has a very limited steering angle, $|\beta_1| \leq 25°$, which limits the curvature of the paths that can be followed with zero steady state tracking error to $|\kappa_\gamma| \leq 0.0022\ \mathrm{mm}^{-1}$ (i.e. $r_\gamma \geq 450$mm). Also for admissible paths, the transient is very often influenced by the saturation in β_1. This is clearly visible in the experiment shown in Fig. 3-4 where the stabilization to an arc of circle is reported. The radius of the reference arc of circle is approx. 500mm i.e. very close to the limit for which an admissible equilibrium exists. The initial off-set is recovered very slowly because of the saturation in β_1. In this case the off-tracking value is easily computed from the steady state values of z_1 and z_3. The controller used in Fig. 3-4 is the high gain output feedback (14). Having used instead the tracking criterion (20), the controller (21) would have kept the whole vehicle outside the reference path in Fig. 3.

References

[1] C. Altafini. A path tracking criterion for an LHD articulated vehicle. *International Journal of Robotics Research*, 18(5):435–441, May 1999.

[2] C. Altafini. Some properties of the general n-trailer. *International Journal of Control*, 74(4):409–424, March 2001.

[3] C. Altafini. Following a path of varying curvature as an output regulation problem. *IEEE Transaction on Automatic Control*, 47(9):1551–1556, 2002.

[4] C. Altafini and P. Gutman. Path following with reduced off-tracking for the n-trailer system. In *Proc. of the 37th Conference on Decision and Control*, pages 3123–3128, Tampa, FL, December 1998.

[5] C. Altafini, A. Speranzon, and B. Wahlberg. A feedback control scheme for reversing a truck and trailer vehicle. *IEEE Transaction on Robotics and Automation*, 17(6):915–922, 2001.

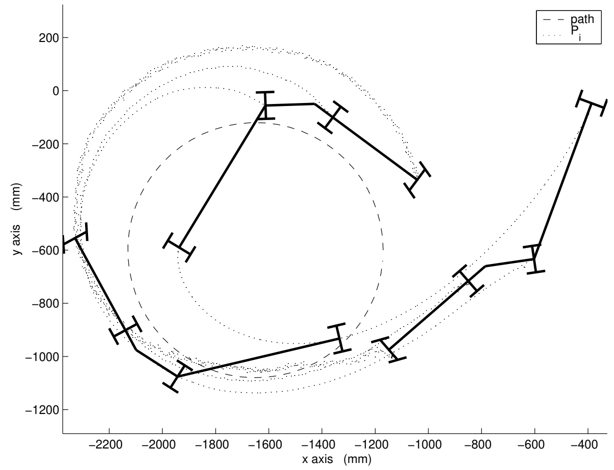

Fig. 3. The multibody vehicle of Fig. 2 following an arc of circle.

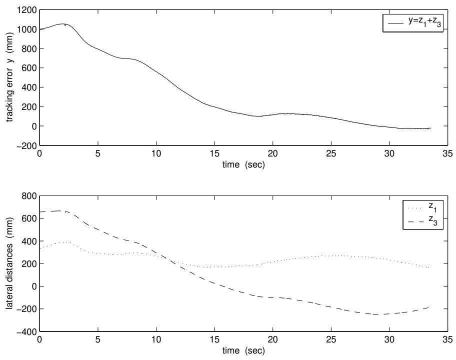

(a) Tracking error y (top) and lateral distances z_1 and z_3 (bottom)

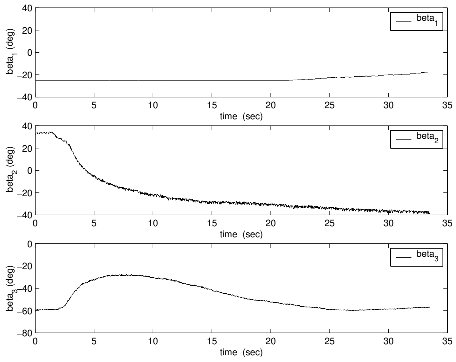

(b) relative angles β_1, β_2 and β_3

Fig. 4. Lateral distances and relative angles for the maneuver of Fig. 3.

[6] P. Bolzern, R. DeSanctis, A. Localtelli, and D. Masciocchi. Path-tracking for articulated vehicles with off-axle hitching. *IEEE Transaction on Control Systems Technology*, 6:515–523, July 1998.

[7] L. Bushnell. An obstacle avoidance algorithm for a car pulling trailers with off-axle hitching. In *Proc. of the Conference on Decision and Control*, pages 3837–3842, New Orleans, LA, 1995.

[8] C. Canudas de Wit. Trends in mobile robot and vehicle control. In K. Valavanis and B. Siciliano, editors, *Control problems in robotics*, Lecture notes in control and information sciences. Springer-Verlag, London, UK, 1998.

[9] C. Canudas de Wit, B. Siciliano, and G. Bastin, editors. *Theory of robot control*. Springer-Verlag, London, UK, 1997.

[10] P. I. Corke and P. Ridley. Steering kinematics for a center-articulated mobile robot. *IEEE Trans. on Robotics and Automation*, 17:215–218, 2001.

[11] M. Fliess, J. Levine, P. Martin, and P. Rouchon. Design of trajectory stabilizing feedback for driftless flat systems. In *Proc. of the 3rd European Control Conference*, pages 1882–1887, Rome, Italy, September 1995.

[12] M. Fliess, J. Levine, P. Martin, and P. Rouchon. Flatness and defect of nonlinear systems: introductory theory and examples. *Int. Journal of Control*, 61(6):1327–1361, 1995.

[13] R. Frezza and G. Picci. On line path following by recursive spline updating. In *Proc. of the Conference on Decision and Control*, pages 4047–4052, New Orleans, LA, 1995.

[14] T. J. Graettinger and B. H. Krogh. Evaluation and time-scaling of trajectories for wheeled mobile robots. *ASME J. of Dynamic Systems, Meas. and Control*, 111:222–231, 1989.

[15] J. Guldner, W.Sienel, J. Ackermann, S. Patwardhan, H. S. Tan, and T. Bünte. Robust control design for automatic steering based on feedback of front and tail lateral displacement. In *Proc. of the 4th European Control Conference*, Brussels, Belgium, 1997.

[16] Y. Kanayama, Y. Kimura, F. Miyazaki, and T. Noguchi. A stable tracking control method for an autonomous robot. In *Proc. 1990 Int. Conf. on Robotics and Automation*, volume 1, pages 384–389, 1990.

[17] D. Lizarraga, P. Morin, and C. Samson. Exponential stabilization of of certain configurations of the general n-trailer system. In *IFAC Workshop on Motion Control*, Grenoble, France, September 1998.

[18] A. Micaelli and C. Samson. Trajectory tracking for unicycle-type and two-steering-wheels mobile robots. Technical Report 2097, INRIA, November 1993.

[19] M. Sampei and K. Furuda. On time scaling for nonlinear systems: Application to linearization. *IEEE Trans. on Automatic Control*, 31:459–462, 1986.

[20] C. Samson. Control of chained systems: application to path-following and time-varying point stabilization of mobile robots. *IEEE Trans. on Automatic Control*, 40:64–77, 1995.

[21] O. J. Sørdalen. Conversion of the kinematics of a car with n trailers into chained form. In *Proc. IEEE Int. Conf. on Robotics and Automation*, pages 382–387, Atlanta, Georgia, 1993.

[22] G. Walsh, D. Tilbury, S. Sastry, R. Murray, and J. Laumond. Stabilization of trajectories for systems with nonholonomic constraints. *IEEE Trans. on Automatic Control*, 39:216–222, 1994.

Appendix

I. Proof of Proposition 2

Just like is Section III-A, also the zero dynamics lacks an analytically computable Jacobian linearization. However, we can use the physical insight in the process to draw conclusions about its stability. Consider the system obtained by choosing $\omega = 0$ in (2): if the initial condition for β_1 is $\neq 0$ and $v_n > 0$, then this corresponds in $\mathcal{D}$ to the n-trailer moving forward with constant steering angle since $\dot{\beta}_1 = 0$. Regardless of the initial condition in $\mathcal{D}$, the system $\dot{\boldsymbol{p}} = \mathcal{F}(\boldsymbol{p})$ tends to move along circular trajectories whose radius is uniquely decided by the initial value of β_1. Restrict to circles that are concentric with the reference trajectory γ; if not, translate γ opportunely. Furthermore, since the path following problem is concerned with stabilization along a path and not around a point, the rate of convergence to the equilibrium is exponential (see [20], [9]). In fact, assuming the contrary means saying that the linearization (which, again, cannot be computed explicitly) is only stable but not asymptotically stable. Then different initial conditions in states other than β_1 would correspond to different equilibrium points, which is against the uniqueness of the solution of an equation similar to (17)

$$y_e = \sum_{i=0}^{n} z_{i_e} = \sum_{i=0}^{n} (r_\gamma - r_i) = const$$

valid for circular equilibrium trajectories concentric to γ. Replacing $\dot{\boldsymbol{p}} = \mathcal{F}(\boldsymbol{p})$ with the zero dynamics of the system means considering the input-output linearizing nonlinear state feedback in place of $\omega = 0$ and pairing the closed loop system $\dot{\boldsymbol{p}} = \mathcal{F}(\boldsymbol{p}) - \mathcal{G}\frac{L^2_{\mathcal{F}}\mathcal{H}\boldsymbol{p}}{L_{\mathcal{G}}L_{\mathcal{F}}\mathcal{H}\boldsymbol{p}}$ with the constraints $y = \dot{y} = 0$. Since ω is entering only in the differential equations for $\dot{\tilde{\theta}}_0$ and $\dot{\beta}_1$, we need to check the asymptotic character of these two only. If we can prove this, then the modified dynamics in β_1 and $\tilde{\theta}_0$ due to the feedback can be thought of as a perturbation on the $\mathfrak{p}$-subsystem, not altering its exponentially convergent character.

Concerning $\tilde{\theta}_0$, it could be concluded directly from (23) and by looking at the expression (18) for the equilibrium point: locally $\tilde{\theta}_i \simeq 0$ while β_i and z_i lie in neighborhoods of nonzero values. Thus, as $\tilde{\theta}_i \to 0$, $i = 1, \ldots, n$, also $\tilde{\theta}_0$ must converge to zero with the same rate. Concerning β_1, its differential equation is $\dot{\beta}_1 = -\frac{L^2_{\mathcal{F}}\mathcal{H}\boldsymbol{p}}{L_{\mathcal{G}}L_{\mathcal{F}}\mathcal{H}\boldsymbol{p}}$. The denominator $L_{\mathcal{G}}L_{\mathcal{F}}\mathcal{H}\boldsymbol{p} = \cos\tilde{\theta}_0 + \sin\tilde{\theta}_0\cos\beta_1$ is locally well-defined and it is positive; the numerator, from the expression of $\ddot{y}$ in [3], p.1553, is

$$L^2_{\mathcal{F}}\mathcal{H}\boldsymbol{p} = L_{\mathcal{F}}\left(\sum_{i=1}^{n} v_i \sin\tilde{\theta}_i\right) + v_0^2\cos\tilde{\theta}_0\left(\frac{\sin\beta_1}{L_1} - \frac{\cos\tilde{\theta}_0\kappa_\gamma(s_{\gamma_0})}{1-\kappa_\gamma(s_{\gamma_0})z_0}\right)$$

where v_i are given by (5). Expanding and isolating the terms containing β_1:

$$\begin{aligned} L^2_{\mathcal{F}}\mathcal{H}\boldsymbol{p} = & \sum_{i=2}^{n}\left(L_{\mathcal{F}}(v_i)\sin\tilde{\theta}_i + v_i\cos\tilde{\theta}_i\dot{\tilde{\theta}}_i\right) + L_{\mathcal{F}}(v_1)\sin\tilde{\theta}_1 \\ & + v_1^2\cos\tilde{\theta}_1\left(\frac{\tan\beta_1}{L_1} - \frac{\cos\tilde{\theta}_1\,\kappa_\gamma(s_{\gamma_1})}{1-\kappa_\gamma(s_{\gamma_1})z_1}\right) \\ & + v_0^2\cos\tilde{\theta}_0\left(\frac{\sin\beta_1}{L_1} - \frac{\cos\tilde{\theta}_0\kappa_\gamma(s_{\gamma_0})}{1-\kappa_\gamma(s_{\gamma_0})z_0}\right) \end{aligned} \quad (29)$$

The $L_{\mathcal{F}}(v_i)$ have a "triangular" structure

$$\begin{aligned} \textstyle\sum_{i=1}^{n} L_{\mathcal{F}}(v_i)\sin\tilde{\theta}_i &= \textstyle\sum_{j=0}^{m}\sum_{i=1}^{n_j+1-n_j} L_{\mathcal{F}}(v_{n_j+i})\sin\tilde{\theta}_{n_j+i} \\ &= \textstyle\sum_{j=0}^{m}\sum_{i=1}^{n_j+1-n_j}\left(\sum_{l=n_j+i+1}^{n}\frac{\partial v_{n_j+i}}{\partial\beta_l}\dot{\beta}_l\right)\sin\tilde{\theta}_{n_j+i} \end{aligned}$$

where

- if $l = n_k$ for some $k > j$ (axle preceding the kingpin hitching) and $l > n_j + i$

$$\frac{\partial v_{n_j+i}}{\partial\beta_l} = v_{n_j+i}\frac{\tan\beta_l - \frac{M_l}{L_l}\tan\beta_{l+1}}{1+\frac{M_l}{L_l}\tan\beta_l\tan\beta_{l+1}}$$

- if $l = n_k + 1$ for some $k > j$ (axle following the kingpin hitching) and $l > n_j + i$

$$\frac{\partial v_{n_j+i}}{\partial\beta_l} = v_{n_j+i}\frac{\tan\beta_l - \frac{M_{l-1}}{L_{l-1}}\tan\beta_{l-1}}{1+\frac{M_{l-1}}{L_{l-1}}\tan\beta_l\tan\beta_{l-1}}$$

- if $l \neq n_j$ and $l \neq n_j + 1$ $\forall j = 0, \ldots, m$

$$\frac{\partial v_{n_j+i}}{\partial\beta_l} = v_{n_j+i}\tan\beta_l$$

Thus $L_{\mathcal{F}}(v_i)$ introduce terms whose denominators are all locally nonnull. Furthermore, all these terms appear multiplied by some $\sin\tilde{\theta}_i$. Therefore the zero output condition computed in $\mathfrak{p}_e$, $L^2_{\mathcal{F}}\mathcal{H}\boldsymbol{p} = 0$, (corresponding here to the equilibrium point for the steering angle β_1) gives all zero terms in (29) except the last two. Concerning $\tilde{\theta}_0$, if $L^2_{\mathcal{F}}\mathcal{H}\boldsymbol{p} = 0$ then from (7)

$$\dot{\tilde{\theta}}_0 = 0 \iff \frac{\sin\beta_1}{L_1} - \frac{\cos\tilde{\theta}_0\kappa_\gamma(s_{\gamma_0})}{1-\kappa_\gamma(s_{\gamma_0})z_0} = 0$$

and therefore β_{1_e} is obtained from the only term remaining:

$$\frac{\tan\beta_1}{L_1} - \frac{\kappa_\gamma}{1-\kappa_\gamma z_{1_e}} = 0$$

which is exactly the value $\arctan\left(\frac{L_1\kappa_\gamma}{1-\kappa_\gamma z_{1_e}}\right)$ computed in (19). To see that such equilibrium is a stable attractor, consider the equation

$$\dot{\beta}_1 = -\left.\frac{L^2_{\mathcal{F}}\mathcal{H}\boldsymbol{p}}{L_{\mathcal{G}}L_{\mathcal{F}}\mathcal{H}\boldsymbol{p}}\right|_{\mathfrak{p}=\mathfrak{p}_e,\ \tilde{\theta}_0=\tilde{\theta}_{0_e}=0}$$

i.e. when all is at the equilibrium except β_1. In this case

$$\left.\dot{\beta}_1\right|_{\mathfrak{p}=\mathfrak{p}_e,\ \tilde{\theta}_0=\tilde{\theta}_{0_e}=0} = v_1^2\left(\frac{\kappa_\gamma}{1-\kappa_\gamma z_{1_e}} - \frac{\tan\beta_1}{L_1}\right)$$

which is asymptotically stable.

∎